ERDC TR-23-3

US Army Corps
of Engineers®
Engineer Research and
Development Center

ERDC
ENGINEER RESEARCH & DEVELOPMENT CENTER

Unconventional Countermeasures for Enhanced Survivability (DeUCES)

Characterization of Pigmented Microbial Isolates for Use in Material Applications

Elizabeth J. Corriveau, Travis L. Thornell, Mine G. Ucak-Astarlioglu, Dane N. Wedgeworth, Hayden A. Hanna, Robert M. Jones, Alison K. Thurston, and Robyn A. Barbato

March 2023

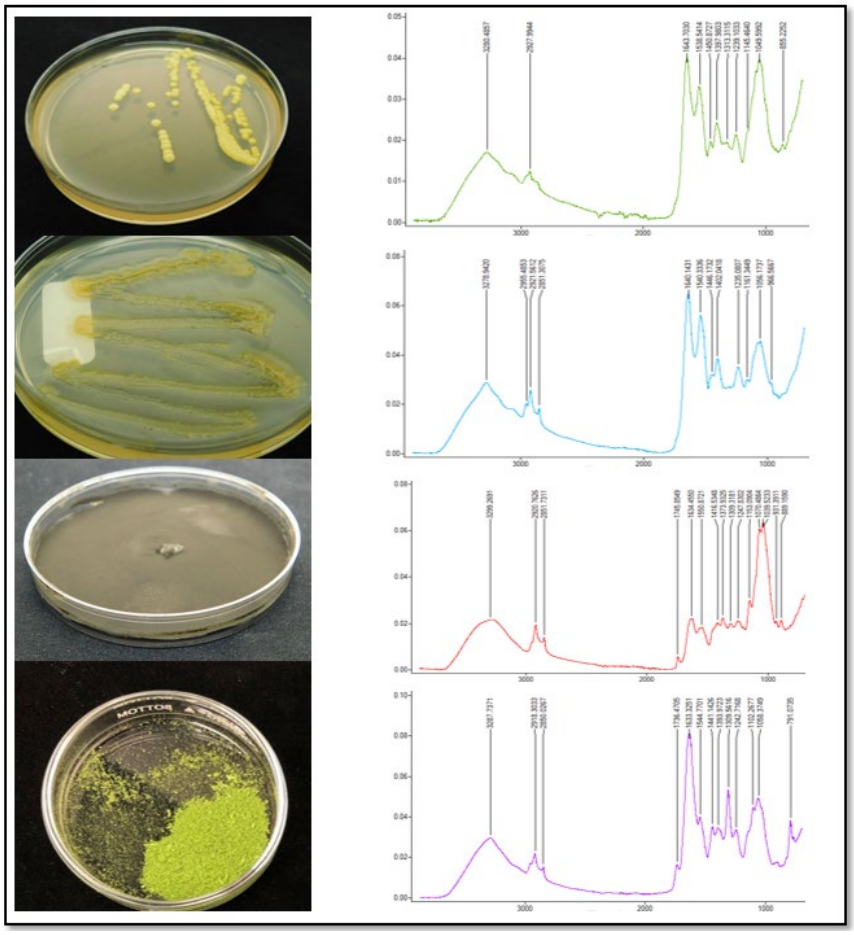

Engineer Research and Development Center

The US Army Engineer Research and Development Center (ERDC) solves the nation's toughest engineering and environmental challenges. ERDC develops innovative solutions in civil and military engineering, geospatial sciences, water resources, and environmental sciences for the Army, the Department of Defense, civilian agencies, and our nation's public good. Find out more at www.erdc.usace.army.mil.

To search for other technical reports published by ERDC, visit the ERDC online library at https://erdclibrary.on.worldcat.org/discovery.

Characterization of Pigmented Microbial Isolates for Use in Material Applications

Elizabeth J. Corriveau, Robert M. Jones, Alison K. Thurston, and Robyn A. Barbato

US Army Engineer Research and Development Center (ERDC)
Cold Regions Research and Engineering Laboratory (CRREL)
72 Lyme Road
Hanover, NH 03755-1290

Travis L. Thornell, Mine G. Ucak-Astarlioglu, Dane N. Wedgeworth, and Hayden A. Hanna

US Army Engineer Research and Development Center (ERDC)
Geotechnical and Structures Laboratory (GSL)
3909 Halls Ferry Road
Vicksburg, MS 39180-6199

Final Report

Prepared for Headquarters, US Army Corps of Engineers
Washington, DC 20314-1000

Under Unconventional Countermeasures for Enhanced Survivability (DeUCES), PE 0602144A, Project BN8, Task SBN811, "Pigmented Polymers for Subterfuge in Complex Environments"

Abstract

Organisms (i.e., plants and microorganisms) contain pigments that allow them to adapt and thrive under stressful conditions, such as elevated ultraviolet radiation. The pigments elicit characteristic spectral responses when measured by active and passive sensors. This research study focused on characterizing the spectral response of three organisms and how they compared to background spectral signatures of a complex environment. Specifically, spectra were collected from a fungus, a plant, and two pigmented bacteria, one of which is an extremophile bacterium. The samples were measured using Fourier transform infrared spectroscopy and discriminated using chemometric means. A top-down examination of the spectral data revealed that organisms could be discriminated from one another through principal component analysis (PCA). Furthermore, there was a strong distinction between the plant and the pigmented microorganisms. Spectral differences resulting in samples with the highest variance from the natural background were identified using PCA loading plots. The outcome of this work is a spectral library of pigmented biological candidates for coatings applications.

Contents

Figures and Tables

Figures

Tables

Preface

This study was conducted for Headquarters, US Army Corps of Engineers, under the Unconventional Countermeasures for Enhanced Survivability (DeUCES), PE 0602144A, Project BN8, Task SBN811, "Pigmented Polymers for Subterfuge in Complex Environments."

The work was performed by the Biogeochemical Sciences Branch of the Research and Engineering Division, US Army Engineer Research and Development Center, Cold Regions Research and Engineering Laboratory (ERDC-CRREL). At the time of publication, Mr. Nate Lamie was branch chief; and Dr. Caitlin A. Callaghan was division chief. Dr. Ivan P. Beckman was acting deputy director of ERDC-CRREL, and Dr. Joseph L. Corriveau was director.

Additional work was performed by the Concrete and Materials Branch of the Engineering Systems and Materials Division, US Army Engineer Research and Development Center, Geotechnical and Structures Laboratory (ERDC-GSL). At the time of publication, Dr. Jameson Shannon was branch chief; and Mr. Justin S. Strickler was division chief. Dr. Matthew D. Smith was the technical director for Civil Works. The deputy director of ERDC-GSL was Mr. Charles W. Ertle II, and the director was Mr. Bartley P. Durst.

Portions of this report's text have been modified and reprinted from R. M. Jones, E. V. Barnes, A. K. Thurston, and R. A. Barbato, *Evaluating the Conductive Properties of Melanin-Producing Fungus,* Curvularia lunata*, after Copper Doping*, ERDC TR-20-25 (Hanover, NH: US Engineer Research and Development Center, 2020), http://dx.doi.org/10.21079/11681/38641. Public domain.

COL Christian Patterson was commander of ERDC, and Dr. David W. Pittman was the director.

This page intentionally left blank.

1 Introduction

1.1 Background

1.1.1 Organisms with unique properties

Natural selection from environmental pressures create new microbiological processes and products (e.g., bacteria and fungi) that enable them to adapt and survive in extreme environments (Cavicchioli et al. 2002). The cold biosphere requires a myriad of synergistic adaptions, resulting in unique structures and functions that could reveal novel products for use in novel material applications. For example, membrane fluidity can be regulated in low temperatures through homeoviscous adaptation, which is done by altering the composition of fatty acids in the lipid bilayer (Hamdan 2018).

With low temperatures also comes ice formation, which can lead to cryoinjury, osmotic stress, dehydration, and cell death. Antifreeze proteins (AFPs) are noncolligative ice-binding proteins that can decrease the freezing point of water and inhibit ice growth. Because of these cryoprotective functions, AFPs are of interest in material sciences for use in surface coating materials to prevent ice formation (Collins and Margesin 2019; Asenath-Smith et al. 2022). Duman and Olsen (1993) were the first to discover the presence of AFPs in bacteria adapted to low temperatures. The Antarctic strain of bacterium *Moraxella* sp. was the first reported to produce an AFP (Dunman and Olsen 1993; Yamashita et al. 2002).

High UV levels are common in cold habitats due to high altitudes or elevations where solar radiation penetrates a thinner atmosphere and snow albedo increases the UV exposure. Pigments, in addition to playing a role in modulation of cell membrane fluidity, provide photoprotection by acting as light screeners protecting against UV radiation (Collins and Margesin 2019). For example, psychrophiles are microorganisms that optimally grow at 15°C or lower (Morita 1975). Pigments are common to psychrophiles, especially those in snow and on glaciers, as they protect cellular components against UV radiation and antioxidants and enable photosynthesis (Dial et al. 2018; Lutz et al. 2015). Specific carotenoid pigments are commonly found in psychrophiles and examples have been reported in various bacteria isolated from Antarctic sea ice (Hamdan 2018).

In material applications, microbial pigments have a wide range of applications in food, drug, colorant, dye, and imaging. Currently, synthetic pigments are widely used globally due to their high production, high intensity, and low cost. However, there is an increasing demand for natural pigments over synthetic pigments, as synthetic pigments have been shown to have negative side effects on human health (e.g., teratogen cancer, etc.). Synthetic pigments are also often not biodegradable, which means they do not break down easily in the environment. This can lead to accumulation of synthetic pigments in the environment and can cause harm to aquatic organisms and humans. Rather than developing synthetic pigments and ways to break them down, it is beneficial to instead research microbial pigments and find potential industrial applications (Chatragadda and Dufossé 2021).

1.1.2 Important traits of pigmented organisms

Carotenoids are a chemically diverse (more than 600 different compounds) class of pigments found in plants, mosses, algae, fungi, and nonphotosynthetic and photosynthetic bacteria. Carotenoids are a class of compounds derived from isoprene units and have a characteristic structure that includes a chain of 3 to 15 double bonds that are conjugated. These conjugated double bonds result in the characteristic absorption found in carotenoids (Nupur et al. 2016). Carotenoids have a variety of roles, including UV radiation defender, solar energy harvester, oxidation inhibitor, immune system modulator, free-radical scavenger, and provitamin A activity. Carotenoids can be divided into two categories: xanthophylls, which contain oxygen, and carotenes, which are composed solely of hydrocarbons without oxygen. These compounds are often lipophilic, meaning they dissolve easily in fats and oils, due to their long unsaturated hydrocarbon chains similar to those found in certain types of fatty acids (Mussagy et al. 2019).

Melanins are a group of pigmented biomacromolecules that are found ubiquitously throughout the biosphere and are resistant to most methods of chemical analysis due to their insolubility. There are three primary types of melanin—eumelanin, pheomelanin, and neuromelanin (Figure 1)—found in animals, plants, bacteria, and fungi. One of the primary roles of melanin is to protect against radiation. Eumelanin, characterized by its dark brown to black coloration, is the most common and has been demonstrated to efficiently block UV (Stein 1955) and gamma radiation (Cordero and Casadevall 2017).

Figure 1. Proposed structures of primary types of melanin: (*A*) eumelanin, (*B*) pheomelanin, and (*C*) neuromelanin. *Arrows* indicate potential attachment sites to other melanin molecules. (Image reproduced from Jones et al. 2020 [public domain], adapted from Ito and Wakamatsu 2008.)

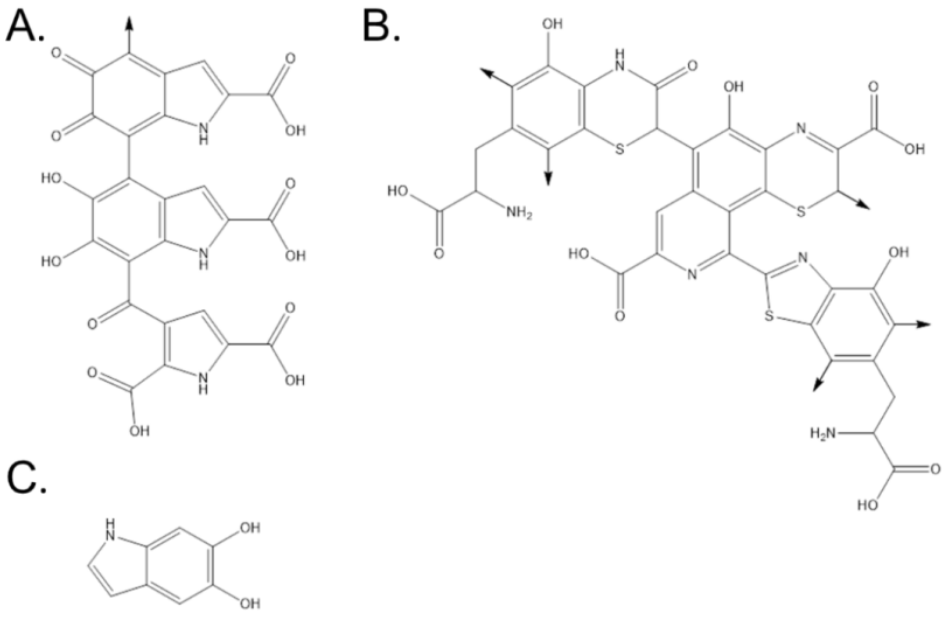

While most color in nature is due to pigment molecules absorbing and reflecting light, there are also occurrences of structural pigmentation, which is caused by light interacting with physical structures that are periodically arranged on a micro- and submicroscale. Light-wave interference with these structures produces iridescence, which is a type of structural coloration that occurs when light waves interact with these structures and causes the color to appear to change as the angle of view or illumination is altered.

1.1.3 Ways to spectrally characterize pigmented microorganisms

Many objects have a material coating that impacts the way the object's surface interacts with electromagnetic radiation (EMR). An example of a common coating is colored paint on walls of infrastructure. These commercially available paints contain various components such as pigments, binders, solvents, surfactants, and other additional additives. The perception of color is caused by pigments (i.e., chlorophyll, carotenoids, and phycobilins), which are molecules that can absorb light in the 13,333–

26,315 cm^{-1} range,* also known as biochromes (Britton 1983). Pigments contain chemical functional groups that can delocalize electrons; and when struck by visible light (14,285–25,000 cm^{-1}), certain wavelengths are absorbed. The human eye detects the ones that are reflected rather than absorbed, and the colors are interpreted by the brain.

EMR can also be detected by remote sensing through observations of radiant energy reflected or emitted by a pigmented object. Remote sensing by definition is the process of obtaining information about an object or area through the use of a device that is not in direct contact with it (Cracknell and Hayes 2007). In addition, there are two types of remote-sensing instruments—passive and active. Passive sensors do not emit any energy of their own and rely on natural or artificial sources of radiation to detect reflection from the Earth's surface and typically record electromagnetic waves in the visible and near-infrared (10,526–13,333 cm^{-1}) ranges. Passive sensors, like cameras, microphones, and radiometers, are utilized in a range of applications such as surveillance, and environmental monitoring. Other passive sensor systems, like SPOT 5 (Satellite Pour l'Observation de la Terre or "Satellite for observation of Earth"), are specifically engineered to capture detailed images of the earth's surface in the middle-infrared wavelengths (5,714–6,329 cm^{-1}). Additionally, thermal remote sensing, which detects radiation naturally emitted by all objects above absolute zero (–273.15°C), is also considered a form of passive remote sensing (Reese et al. 2013). In contrast to passive sensors, active sensors emit energy to detect and measure information about a target. Different types of active sensors operate at various ranges of the electromagnetic spectrum (EMS). For instance, radar uses microwaves, lidar uses visible, near-infrared, and infrared light, and sonar uses sound waves to detect and measure information (Zhu et al. 2018). Military advancements in passive and active remote-sensing technologies have resulted in high-resolution change detection in complex environments, making critical defense assets easily targeted. The region of the EMS that is of interest for this research includes midwave infrared (MWIR; 1,250–3,333cm^{-1}) and long-wave infrared (LWIR; 700–1,250 cm^{-1}; Dereniak and Boreman 1996) due to the common use of remote detection of thermal radiation emitted from all objects. Included in this phenomenon are microorganisms, which have

* For a full list of the spelled-out forms of the units of measure used in this document, please refer to *US Government Publishing Office Style Manual*, 31st ed. (Washington, DC: US Government Publishing Office, 2016), 248–252, https://www.govinfo.gov/content/pkg/GPO-STYLEMANUAL-2016/pdf/GPO-STYLEMANUAL-2016.pdf.

varying chemical components that produce spectral responses unique down the subspecies level in the infrared (IR) region of the electromagnetic spectrum (IR; Table 1).*

Table 1. Characteristic bands of biological functional groups detected using FTIR (adapted from Davis and Mauer 2010; Schmitt and Flemming 1998).

Wavenumber (cm^{-1})	Band Assignment
3,400	OH of water
2,956	CH_3 asymmetrical stretch in fatty acids
2,920	CH_2 asymmetrical stretch in fatty acids
2,898	C–H stretching in the C–H of amino acids
2,870	CH_3 symmetrical stretch in fatty acids
2,850	CH_2 symmetrical stretch in fatty acids
1,740	C=O stretch of lipid ester
1,705	C=O stretch of ester in nucleic acids and carbonic acids
1,695–1,675	Amide I, (C=O) protein components
1,655	Amide I of α-helical structures of proteins
1,637	Amide I of β-pleated sheet structures of proteins
1,550–1,520	Amide II, N–H, C–N, and structure of proteins
1,515	Tyrosine band
1,460–1,454	C–H bend from CH_2 in lipids proteins
1,415	C–O–H in-plane bending in carbohydrates, DNA/RNA backbone, proteins
1,400	C=O symmetric stretching of COO group in amino acids and fatty acids
1,310–1,240	Amide III band components of proteins
1,240	P=O from phosphate
1,200–900	C–O–C, C–O dominated by ring vibrations in various polysaccharides
1,114	C–O–P, P–O–P
1,085	P=O symmetric stretching in DNA, RNA, and phospholipids
720	C–H rocking of CH_2 in fatty acids

Fourier transform infrared (FTIR) spectroscopy of organisms reveals important information on functional groups of proteins, fatty acids, carbohydrates, nucleic acids, and lipopolysaccharides (Table 1; Davis and Mauer 2010; Schmitt and Flemming 1998). The work herein uses attenuated total reflectance FTIR (ATR-FTIR; 700–4,000 cm^{-1}) to image the chemical composition of selected pigmented organisms in the IR and uses

* For a full list of the spelled-out forms of the chemical elements used in this document, please refer to *US Government Publishing Office Style Manual*, 31st ed. (Washington, DC: US Government Publishing Office, 2016), 265, https://www.govinfo.gov/content/pkg/GPO-STYLEMANUAL-2016/pdf/GPO-STYLEMANUAL-2016.pdf.

chemometrics to determine similarities between the pigmented organisms and vegetation. This data analysis was used to down select for microbes of potential interest to be later used with advanced material coatings to alter the surface of objects to match that of more complex natural backgrounds (i.e., vegetation) in the IR wavelength range.

1.2 Objectives

The goal of this research was to develop a pipeline to screen and identify biological candidates that may serve as spectrally selective biological additives to embed in material coatings that could be detected through standoff-sensing means. The specific aims include adapting existing methods to pellet lyophilized biomass from candidate organisms, assessing their spectral properties, and comparing the spectra to that of vegetation. The following were our three main objectives:

- Identify three candidate pigmented microbes with various pigment strategies (i.e., melanin, carotenoid, or structural pigments) sourced either through isolation from cold regions samples in the US Army Cold Regions Research and Engineering Laboratory (CRREL) Innovative, Collaborative, Exploratory Cold Regions Organismal Library for Discovery (ICE-COLD) or purchased from ATCC (American Type Culture Collection).
- Assess pigmented candidates as potential spectrally selective additives through biochemical phenotyping of pelleted whole cells by using FTIR.
- Statistically compare the three pigmented organism's spectra using principal component analysis (PCA) methods to discriminate and characterize the biological candidates and compare them to spectra from a complex background.

1.3 Approach

This study used infrared spectroscopy, a well-established method, to recognize functional groups in microorganisms through examining their vibration modes at various infrared wavelengths (Ojeda and Dittrich 2012). Nondestructive measurements of samples were made using the ATR spectroscopic reflection technique, which uses internal total reflectance and requires minimal sample preparation. The measurement quality of the technique depends strongly on direct contact between the samples and the ATR crystal (Smith 2011). When working with solids or powders

using this methodology, the sample must be clamped down for even contact with the ATR crystal. To achieve this, biomass was collected and combined with potassium bromide (KBr) and pelleted.

Further analysis of the IR data consisted of performing PCA on the full data set and on regions of interest associated with remote sensors. The PCA models produced showed clustering based on sample similarity, with each plot point representing a spectral scan. PCA loading plots were then derived from the principal components, which indicate the spectral regions responsible for segregation in the PCA (Hanson 2012).

2 Methods

2.1 Bacterial and fungal candidate selection

Because of its carotenoid pigmentation, Cold Isolate 1 (ICE-COLD catalog number IE3-IE3-TSA-25-D-I1) was selected as a candidate in this study. Cold Isolate 1 is a gram-positive bacterial isolate from the CRREL ICE-COLD Library. Cold Isolate 1 was isolated from Greenland ice growing in the light at 25°C with observed growth temperatures as low as 4°C. Attractive characteristics include its ability to grow rapidly with a doubling time of 2.2 hours, robustness of the cells observed in various growth conditions, and bright yellow appearance (Figure 2) from carotenoid pigmentation. Cold Isolate 1 has a cocci bacterial shape, growing mostly in pairs with round colonies that get more intense in color as the colonies grow larger.

Figure 2. Bright-yellow colonies of Cold Isolate 1. The figure on the *right* is a general structure of a carotenoid, which is responsible for the yellow pigmentation seen in Cold Isolate 1. (*Right* image reproduced from Ben Mills, *Isorenieratene 2D Skeletal*, 2009, https://en.wikipedia.org/wiki/Carotenoid. Public domain.)

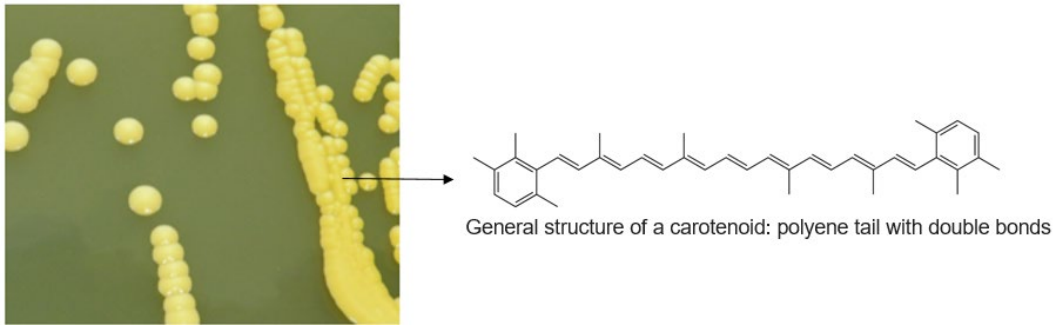

Cellulophaga lytica was selected for this research due to its documented production of structural pigmentation when grown under laboratory conditions (Kientz et al. 2016). *C. lytica* is a bacterium that has been isolated from the surfaces of anemone and contains a unique iridescent biofilm, which has shown to strongly reflect wavelengths spanning near-UV, visible, and near-infrared. This iridescent biofilm has potential biological roles such as thermoregulation or photo protection (Kientz et al. 2016); however, iridescence has been inadequately recorded in scientific literature since its first observation, made in 1904 by Preisz (1904). Previously, biotechnological interest in *C. lytica* has focused on its ability to produce a diverse set of extracellular enzymes that can break down proteins and polysaccharides (Pati et al. 2011).

Additionally, *Curvularia lunata* was selected for this research because it can quickly produce dark wooly melanized cultures on potato dextrose agar and because of the role melanin plays in protection against UV, thermal, and high-energy radiation (Turick et al. 2011).

2.2 Bacterial and fungal candidate culturing

2.2.1 Media preparation

Broths were prepared by combing ingredients and dissolving them before they were autoclaved, such that the liquid temperature reached 121°C and 6.9 kPa for at least 25 minutes. To prep plates, agar was added to the broth solutions and prepared in accordance with standard preparation techniques. In brief, ingredients were completely dissolved on a stirring hot plate and then autoclaved using the same parameters as described previously for the broth preparation. Molten agar was then allowed to cool slightly at room temperature before being poured into sterile petri plates.

2.2.2 Candidate propagation and culturing

2.2.2.1 Bacterial culturing

Liquid cultures were necessary for biomass collection for downstream analysis, so using a flame-sterilized stainless-steel inoculation loop, single Cold Isolate 1 colonies were collected from a cultured plate and transferred into six separate 125 mL sterilized flasks containing 75 mL of liquid broth (trypticase soy broth) and covered with sterilized aluminum foil to keep out possible contaminants. The cultures were then shaken at 200 rpm for 48 hours on the benchtop at room temperature.

Celluphaga lytica was purchased from ATCC (ATCC 23178; Johansen et al. 1999). *C. lytica* was received in a dried state and revived following the manufacturer's instructions prior to inoculation on marine agar. Six separate liquid cultures of *C. lytica* were started using the same methodology described for Cold Isolate 1, with the only difference being marine broth was used in place of trypticase soy broth.

2.2.2.2 Fungal culturing

Curvularia lunata was purchased from ATCC (ATCC 42011; Malik et al. 1979). *C. lunata* was received in a dried state and revived following the manufacturer's instructions prior to inoculation on potato dextrose agar

(PDA). Agar plates, rather than liquid, were used for culturing to acquire thick, felt-like mats of melanin. Six PDA plates were inoculated by removing 3 × 3 mm plugs from existing cultures by using a flame-sterilized scalpel and depositing the plug in the center of the PDA plate culture-side down. The plates were then incubated at 28°C in the dark.

2.3 Biomass collection and preparation

The biomass collection and preparation process was different for the bacterial and fungal samples due to the fungal samples growing poorly in liquid broth. For the bacterial samples, *C. lytica* and Cold Isolate 1, cultured broth was placed in a biosafety cabinet (NUAIRE, Class II, type A, Plymouth, Minnesota, USA). The cultured broth of each replicate was carefully poured into a sterile 100 mL conical tube for centrifugation (Thermo Fisher Scientific, Sorvall RC 6, Waltham, Massachusetts, USA) to pellet cells at 20 × g for 10 m at 4°C. The remaining pellet was transferred by pipette into a 2 mL sterile cryopreservation tube. In the 2 mL tube, the samples were centrifuged using the same parameters, and the supernatant was carefully removed with a 200 mL pipette. As a negative control, 1 mL of corresponding broth used for culturing was placed in a 2 mL cryopreservation tube.

For the fungal sample, *C. lunata*, biomass was collected from six separate agar media plates that incubated for at least 10 days to allow for the melanin felt to grow thick enough for removal from the agar. Cultures were scraped off the agar surface using flame-sterilized scalpels and spatulas. Scraped cultures from multiple plates were combined in an autoclaved glass petri plate until processing. The cultures were then put in a sterile stainless-steel mesh filter and washed three times with boiling deionized water to remove any excess agar.

All biomass collected from the fungal and bacterial samples was frozen for at least 4 hours in a −80°C freezer prior to being lyophilized on a VirTis FreezeMobile 12XL (Gardinar, New York, USA) overnight for 12–16 hours. Once samples were dried via lyophilizaton, the *C. lunata* fungal samples were milled using an Ika A11 Basic Analytical Mill (Wilmington, North Carolina, USA) for a total of 60 seconds in 5-second pulses (Jones et al. 2020).

Spinacia oleracea, or more commonly known as spinach, was purchased from the local grocery store and rinsed with deionized water and allowed

to dry in a biosafety cabinet. The clean *S. oleracea* was then frozen for at least 4 hours in a −80°C freezer prior to being lyophilized on a VirTis FreezeMobile 12XL (Gardinar, New York, USA) overnight for 12–16 hours. Once samples were dried via lyophilizaton, they were ground using a pestle and mortar. All bacterial, fungal, and plant samples were stored at 4°C with desiccant until use.

2.4 Pelleting lyophilized biomass in potassium bromide

To prepare the pellets for benchtop ATR-FTIR analysis, lyophilized material was taken from each biological replicate and mixed separately with baked KBr using a pestle and mortar until smooth (Figure 3). The KBr was baked at 110°C for 2–3 hours to remove excess water. Between samples, the pestle and mortar were cleaned with 70% ethanol. After cleaning, the pestle and mortar were allowed to fully dry to avoid lyophilized material from absorbing any liquid water, which would negatively impact the spectral collection. The matrix used to create each pellet is in Table 2.

As shown Figure 4, to prepare the pellets, each lyophilized sample was placed into a 13 mm pellet pressing die and put under 5 tons (4,536 kg) of pressure using a hydraulic hand press (Carver 4350.L, Wabash, Indiana, USA). Once the desired pressure was reached, it was maintained for 3 minutes, after which the pellet was evacuated from the die and stored in a separate sterile Whirl-Pak bag. A total of six pellets were made for each material type (i.e., *C. lunata*, *C. lytica*, Cold Isolate 1, and *S. oleracea*).

Figure 3. Lyophilized biomass and KBr mixed using pestle and mortar.

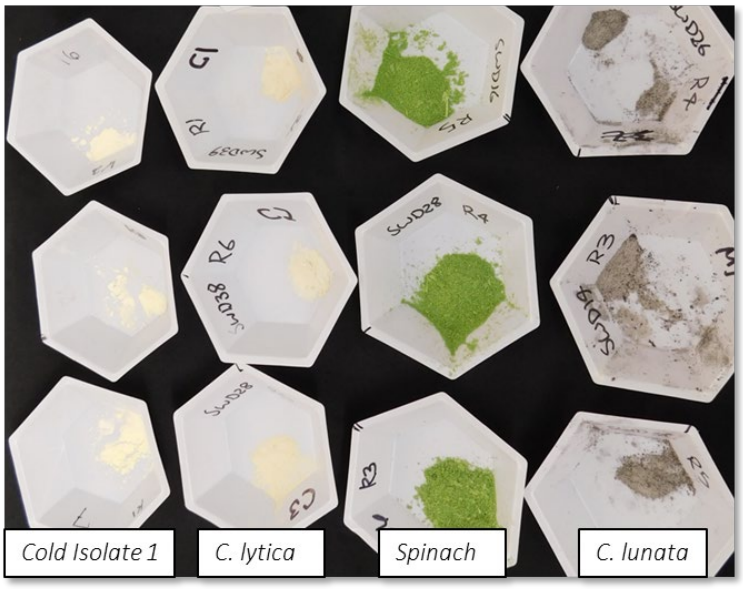

Table 2. Pellet matrix.

Material	Pellet Replicate 1	Pellet Replicate 2	Pellet Replicate 3	Pellet Replicate 4	Pellet Replicate 5	Pellet Replicate 6
S. oleracea Freeze-Dried (g)	0.093	0.071	0.08	0.08	0.071	0.08
KBr (g)	0.137	0.159	0.15	0.15	0.159	0.15
C. lytica Freeze-Dried (g)	0.025	0.03	0.013	0.024	0.013	0.022
KBr (g)	0.205	0.227	0.217	0.206	0.217	0.208
Cold Isolate 1 Freeze-Dried (g)	0.02	0.01	0.03	0.011	0.011	0.007
KBr (g)	0.228	0.229	0.227	0.229	0.219	0.223
C. lunata Freeze-Dried (g)	0.04	0.04	0.04	0.04	0.04	0.04
KBr (g)	0.226	0.226	0.226	0.226	0.226	0.226

Figure 4. Workflow for sample pellet preparation for ATR-FTIR analysis.

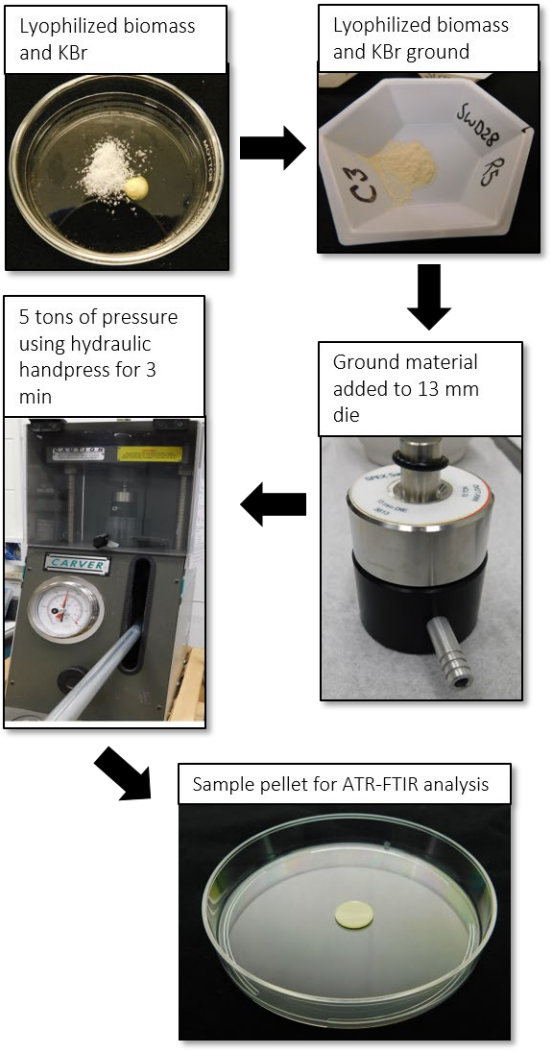

2.5 Spectral analysis using ATR-FTIR (attenuated total reflectance Fourier transform infrared)

2.5.1 Infrared (IR) data acquisition

In this study, ATR-FTIR spectra were obtained by directly placing the pelleted samples on the ATR diamond crystal and clamping them using a pressure gauge. The proper adjustment of the ATR clamp allowed for even distribution of the sample over the crystal surface. The infrared beam was directed onto an optically dense crystal at a 45° angle. The internal reflectance created an evanescent wave that protruded a few microns (0.5–5 µm) beyond the crystal and into the sample. The depth at which the evanescent wave penetrates into the sample is determined by the difference in the refractive index between the sample and the ATR crystal. After the sample absorbed unique regions of the infrared spectrum, the evanescent wave became attenuated. The attenuated energy from the evanescent wave then comes back to the crystal, exits from the opposite end of the crystal, and is then sent to the detector in the IR spectrometer (Figure 5).

Figure 5. Working principles of single reflection ATR-FTIR spectroscopy.

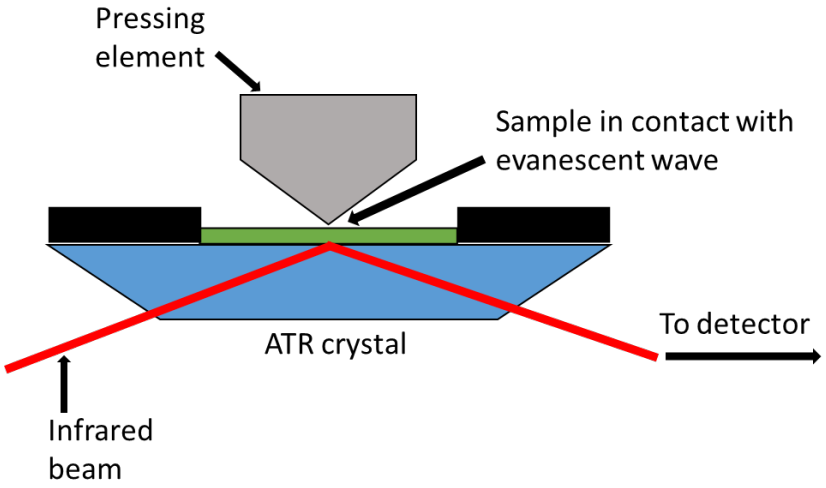

Pellets were scanned on a Nicolet 6700 FTIR (Thermo Fisher Scientific, Waltham, Massachusetts, USA) equipped with the diamond Smart iTR Attenuated Total Reflectance (ATR) Sampling Accessory (Thermo Fisher Scientific, Waltham, Massachusetts, USA) and deuterated triglycine sulfate KBr detector. The samples were placed on the ATR diamond crystal and held in place with the pressure gauges. Each spectral measurement consisted of 32 scans at a resolution of 4 cm^{-1}, and a background scan prior to each sample was performed using a plain KBr pellet to subtract

the background. Before each set of measurement, a polystyrene standard was also run to ensure the instrument was operating as expected. Each biological material sample group had six pellets in total, and each pellet was scanned in duplicate.

The complex background comparison was conducted by collecting background vegetation scans in the afternoon using the hand-held 4300 FTIR (Agilent Technologies, Santa Clara, California, USA) with the ATR accessory and coarse gold reference. The 12 locations chosen had predominantly grass vegetation and were located outside of CRREL, Hanover, New Hampshire. Method parameters for these measurements consisted of four clean scans performed prior to sampling to ensure the diamond crystal was clean, 16 background spectra, and 16 sample scans. The background spectrum includes unwanted spectral contributions from the instrument and environment, such as infrared absorbing water vapor (3,500 cm^{-1} and 1,630 cm^{-1}) and carbon dioxide (2,350 cm^{-1} and 667 cm^{-1}). To remove these unwanted bands and calculate the absorbance spectrum of a sample, the following equation is used (Smith 1996):

$$A = \log (I_0/I),$$

where

A = absorbance,
I_0 = intensity in the background spectrum, and
I = intensity in the sample spectrum.

Data was collected at a resolution of 4 cm^{-1}. The measurements were taken in reflectance and converted to absorbance in Essential FTIR software.

2.5.2 Preprocessing of IR data

The preprocessing of the FTIR data used Essential FTIR software as follows: (1) correct baseline for any dissimilarities between spectra due to baseline deviations, (2) normalize all spectra from all sample sets to the same intensity to remove variations from different amounts of material, and (3) smooth the entire spectra to increase the precision of the data without distorting the signal tendency by using the Savitzky-Golay algorithm, window size 11 (Savitzky and Golay 1964; Mariey et al. 2001). The spectra were then separated out based on regions of interest, including MWIR, LWIR, and the full spectral scan. The absorption and wavelength

data were exported from Essential FTIR as a .csv multifile for statistical analysis.

2.5.3 Statistical analysis of IR data

The processed FTIR spectra were statically compared using PCA in the package Chemospec (Hanson 2012) in R (R Core Team 2017). PCA was employed to decrease the complexity of the data set into its most significant components or scores while retaining the important variation between the data points. PCA loading plots were then derived to indicate the spectral regions responsible for segregation in the PCA (Hanson 2012). Figure 6 shows the workflow for this process.

Figure 6. Workflow from raw ATR-FTIR data to R for exploratory data analysis.

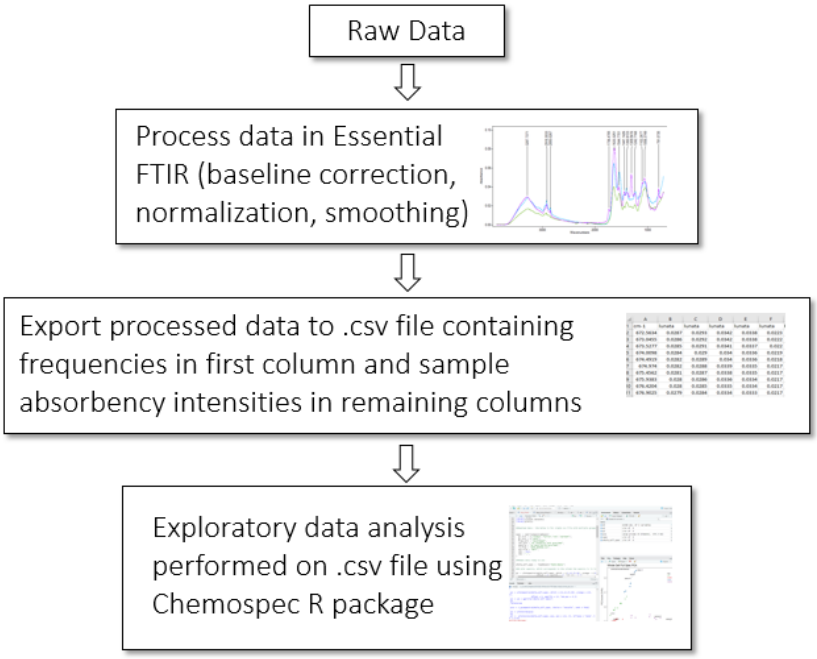

3 Results and Discussion

3.1 ATR-FTIR measurements and analysis

Figure 7 visually compares the spectra of *C. lunata*, *C. lytica*, Cold Isolate 1, *S. oleracea*, and background vegetation. Each spectra represents a single spectrum representative of each sample group. Figure 8 presents all twelve consecutive scans collected from each sample, showing reproducibility between the scans. In general, the location of the peaks representing the structural and functional groups of the molecules were similar and had similar intensities. For instance, each spectrum had a peak near 1,630 cm^{-1}, which is associated with the C=O stretch amide I of proteins.

Figure 7. ATR-FTIR Spectra of (*A*) *C. lunata*, (*B*) *C. lytica*, (*C*) Cold Isolate 1, (*D*) *S. oleracea*, and (*E*) background vegetation.

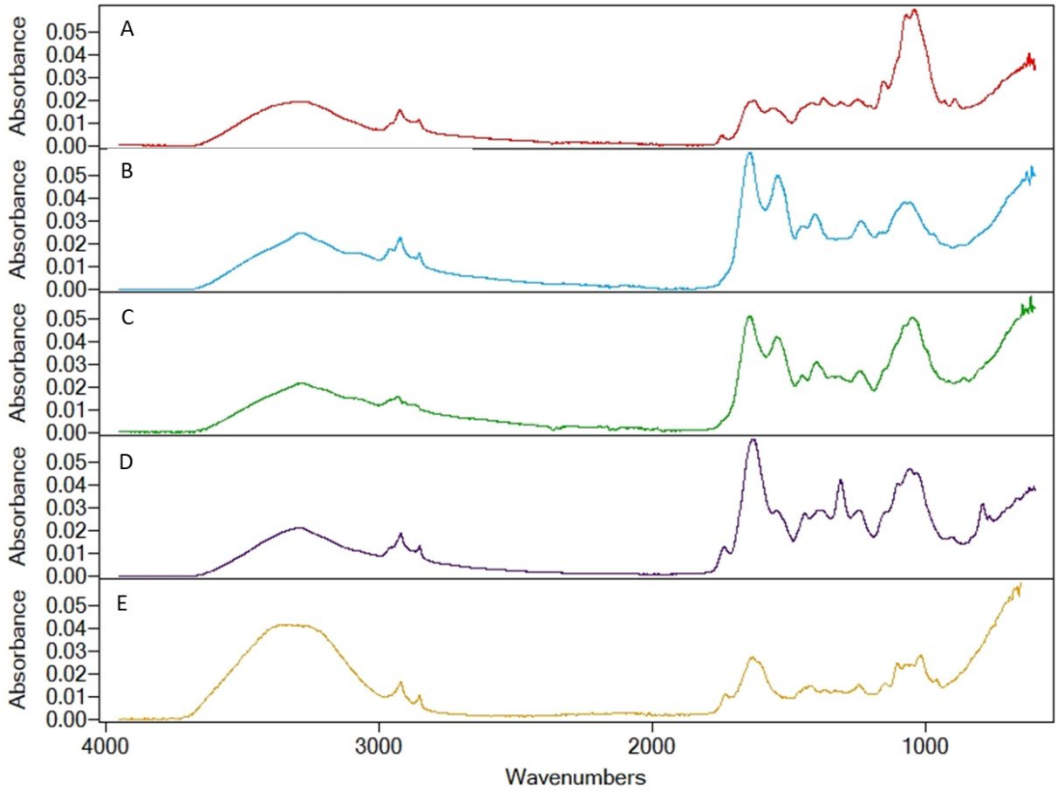

Figure 8. Overlay of ATR-FTIR spectra showing reproducibility for each sample group.

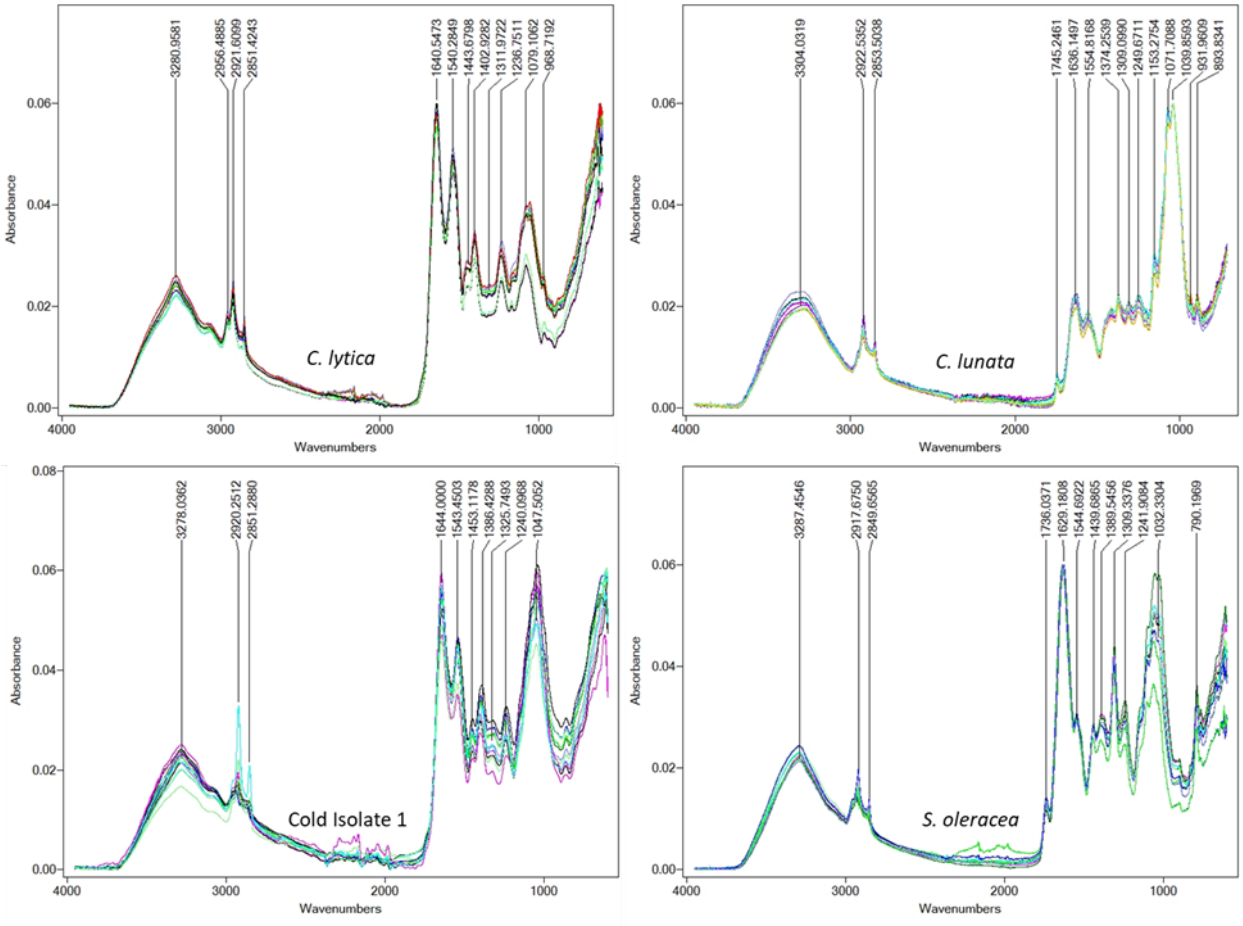

3.2 Statistical analysis of spectra

PCA was used as an ordination technique to compare the organisms to one another and to the complex background. PCA was performed on regions of interest including 667–4,000 cm^{-1} (Figure 9), MWIR region (Figure 10), and LWIR region (Figure 11). Included with each scores plot are the PCA loading plots derived for principle component 1 (PC1) and principle component 2 (PC2), which indicate the spectral regions responsible for segregation along each axis. The loading plots include each frequency in the data; and the higher the intensity (negative or positive), the stronger the impact it had on the final PCA output.

Figure 9. PCA scores plot of ATR-FTIR spectra 667–4,000 cm^{-1} shown on the *right* and the loading plot derived from the PCA showing the spectral bands responsible for the variances in PC1 and PC2.

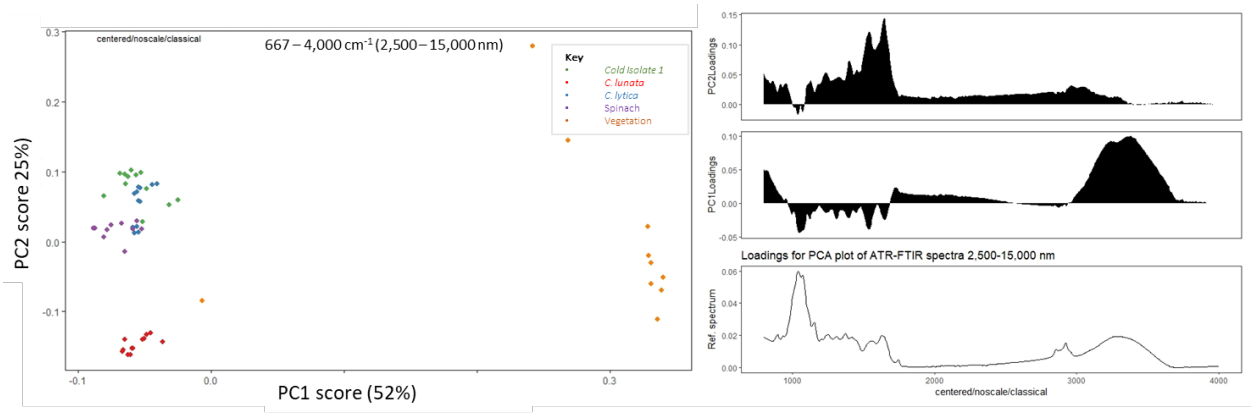

When investigating the spectral region 667–4,000 cm^{-1} (Figure 9) using PCA, the vegetative background is separated from the microbial and *S. oleracea* samples along the PC1 axis, which represents 52% of the total variance. The corresponding loading plots shows PC1 is influenced strongly by a distinct band found between 3,279 and 3,317 cm^{-1}, which is likely due to the vibration of the O–H stretch in water (Schmitt and Flemming 1998). The higher water content present in the natural vegetation compared to the lyophilized microbial and *S. oleracea* pellets is suspected to be the cause for the broader peak found at 3,200 cm^{-1} in the vegetative background, contributing heavily to the segregation of vegetative background from other samples along PC1. Water produces a strong FTIR signal, which can cause other compounds present to go undetected. Separation along PC1 is also influenced by opposing bands for 1,500–1,200 cm^{-1}. Davis and Mauer (2010) reported this region as a major IR region of interest for bacterial identification in samples absent of water due to again the strong FTIR water signals blocking the spectral response from fatty acid bending vibrations, proteins, and phosphate-carrying compounds that are otherwise detectable in the 1,500–1,200 cm^{-1} region (Davis and Mauer 2010). Vegetative background lacked distinctive bands in this region (Figure 7), likely due to the water present in the sample. A unique band in *S. oleracea* was found at 1,309 cm^{-1} and is likely due to the vibrations of C–O of the syringyl ring, which plays a role in the production of lignin (Zhao et al. 2010; Jones et al. 2017).

Along PC2, which represents 25% of the total variance in the data set, *C. lunata* separates from *S. oleracea* and the bacterial samples while appearing slightly more in line with the vegetative background (Figure 9). This suggests that the spectral signature of *C. lunata* is more similar to complex

background samples yet less similar to its bacterial counterparts. Interestingly, the samples of *S. oleracea* clustered with the bacteria rather than the complex background. This might be due to the lack of water found in the dried *S. oleracea* samples, which is present in the complex background, causing a broader peak at 3,200 cm^{-1}. The corresponding loading plot shows PC2 is influenced by the presence of intense bands at about 1,630 cm^{-1} (1,633–1,640 cm^{-1}), which is associated with the C=O stretch amide I of proteins, and between 1,538 and 1,550 cm^{-1}, which is caused by the bending vibrations of N–H in amide II of proteins (Schmitt and Flemming 1998). The vegetative background showed absorption at only 1,630 cm^{-1}, which is likely caused by C=O stretch amide I from protein.

Figure 10. PCA scores plot of ATR-FTIR spectra 1,250–3,333 cm^{-1} shown on the *right* and the loading plot derived from the PCA showing the spectral bands responsible for the variances in PC1 and PC2.

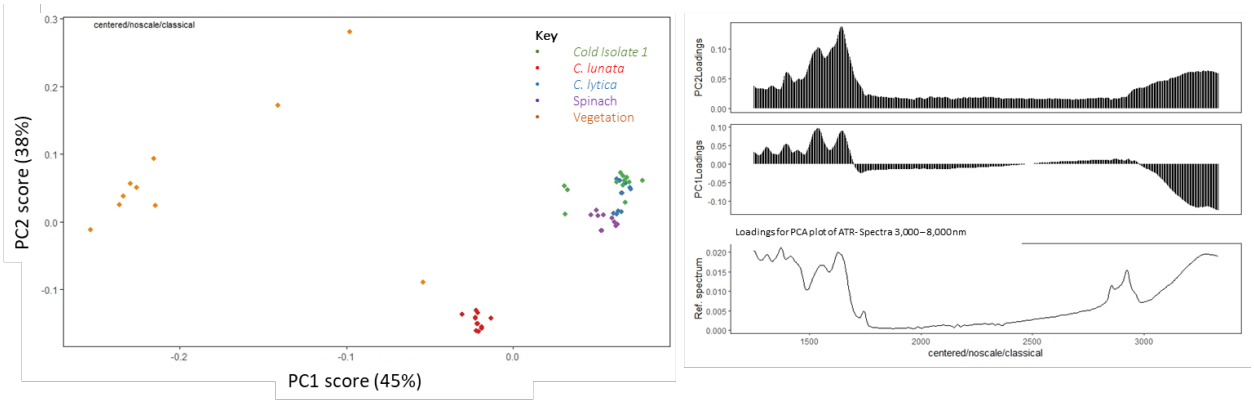

When investigating the MWIR spectral region 1,250–3,333 cm^{-1} (Figure 10) using PCA, the vegetative background is separated from the organismal samples along the PC1 axis, which represents 45% of the total variance. There appears to be a slight shift of *C. lunata* towards the vegetative background along PC1, suggesting that there may be better overlap in spectral similarities between *C. lunata* and the vegetative background in the MWIR.

The corresponding loading plot (Figure 10) shows PC1 has similar spectral regions responsible for segregation along each PC1 axis as the loading plot found in Figure 9 and is also heavily influenced by the water-related band found at about 3,200 cm^{-1}. PC1 and PC2 both appear to be influenced by bands between 1,633 and 1,640 cm^{-1} and between 1,538 and 1,550 cm^{-1} with differences in peak height ratios. PC1 is also influenced by an opposing band found between 1,732 and 1,745 cm^{-1}. The 1,744 cm^{-1} band from

this range is likely caused by the vibrations of the C=O stretch in lipid esters due to this being a characteristic band present in biological functional groups (Table 1) and can be detected in only the *C. lunata*, *S. oleracea*, and vegetative background.

Figure 11. PCA scores plot of ATR-FTIR spectra 700–1,250 cm^{-1} shown on the *right* and the loading plot derived from the PCA showing the spectral bands responsible for the variances in PC1 and PC2.

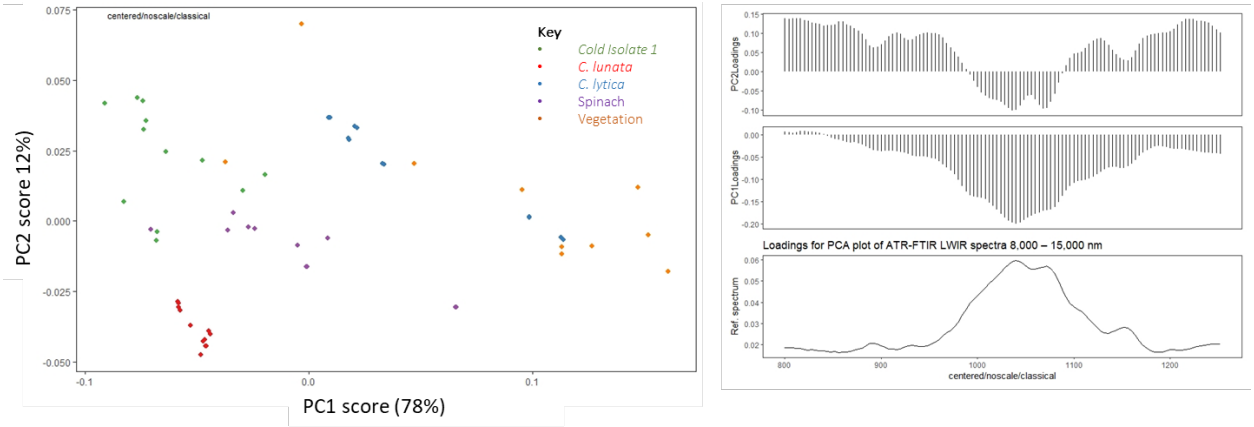

When investigating the LWIR spectral region 700–1,250 cm^{-1} (Figure 11) using PCA, the vegetative background shifts closer to the organismal samples along the PC1 axis, which represents 78% of the total variance. Specifically, along PC1, the vegetative background and *C. lytica* appear closer, meaning there may be better overlap in spectral similarities between *C. lytica* and the vegetative background in the LWIR. The corresponding loading plot (Figure 11) shows that PC1 and PC2 are influenced by a distinct band found at about 900–1,200 cm^{-1} and that this region is dominated by C–O–C, C–O ring vibrations in various polysaccharides (Schmitt and Flemming 1998).

While none of the samples matched outdoor vegetation perfectly, the similarities between spectra due to biological functional groups is apparent. Currently, the CRREL Soil Microbiology group has 42 pigmented bacteria and yeast as part of ICE-COLD, and the PCA analysis process used for this research could potentially screen for microbes of interest. The identification of compatible biomaterials to embed unviable organisms in may also be possible. Investigating the emissivity of biological materials embedded in a coating for outdoors field testing could provide further insight into the effects of EMR on the spectral signature.

4 Conclusion

The spectral signature of complex backgrounds and the spectral signatures of pigmented organisms are of interest to assess candidates for coatings research. Therefore, the goal of this study was to assess organisms with various pigment strategies by using spectroscopic techniques and to statistically compare the signals to that of a natural vegetative background. The statistical comparison between the organism samples and the complex vegetative background indicated that the spectra of the complex vegetative background was different from the organisms tested. This separation is primarily due to the vibration of the O–H stretch of water found in the natural vegetative background scans, which indicates the strong impact water has on the spectral signature of background vegetation. Bands associated with amide I and II protein regions also influenced clustering and were found in Cold Isolate 1, *C. lytica*, and the *S. oleracea* samples. The fungal candidate, *C. lunata*, appeared more similar to the vegetative background in the Amide I and II protein regions. By understanding the functional groups contributing to the differences in the spectra, our team can begin to target scenarios where the candidate combined with the coating would be most effective.

References

Asenath-Smith, Emily, Emily C. Jeng, Emma K. Ambrogi, Garrett R. Hoch, and Jason L. Olivier. 2022. *Investigations into the Ice Crystallization and Freezing Properties of the Antifreeze Protein ApAFP752*. ERDC/CRREL TR-22-17. Hanover, NH: US Army Engineer Research and Development Center, Cold Regions Research and Engineering Laboratory. http://dx.doi.org/10.21079/11681/45620.

Britton, George. 1983. *The Biochemistry of Natural Pigments*. New York: Cambridge University Press.

Cavicchioli, Ricardo, Khawar S. Siddiqui, David Andrews, and Kevin R. Sowers. "Low-Temperature Extremophiles and Their Applications." *Current Opinion in Biotechnology* 13 (3): 253–61. https://doi.org/10.1016/s0958-1669(02)00317-8.

Chatragadda, Ramesh, and Laurent Dufossé. 2021. "Ecological and Biotechnological Aspects of Pigmented Microbes: A Way Forward in Development of Food and Pharmaceutical Grade Pigments." *Microorganisms* 9 (3): 637. https://doi.org/10.3390/microorganisms9030637.

Collins, Tony, and Rosa Margesin. 2019. "Psychrophilic Lifestyles: Mechanisms of Adaptation and Biotechnological Tools." *Applied Microbiology and Biotechnology* 103 (7): 2857–71. https://doi.org/10.1007/s00253-019-09659-5.

Cordero, Radames J. B., and Arturo Casadevall. 2017. "Functions of Fungal Melanin beyond Virulence." *Fungal Biology Reviews* 31 (2): 99–112. https://doi.org/10.1016/j.fbr.2016.12.003.

Cracknell, Arthur P. and Ladson Hayes. 2007. *Introduction to Remote Sensing*. 2nd ed. Boca Raton, FL: CRC Press. https://books.google.com/books?hl=en&lr=&id%0b=oRPNBQAAQBAJ&oi=fnd&pg=PP1&dq=Cracknell.

Davis, Reeta, and Lisa J. Mauer. 2010. "Fourier Transform Infrared (FT-IR) Spectroscopy: A Rapid Tool for Detection and Analysis of Foodborne Pathogenic Bacteria." In *Current Research, Technology and Education Topics in Applied Microbiology and Microbial Biotechnology*, edited by A. Méndez-Vilas, 1582–94. Badajoz, Spain: Formatex Research Center.

Dereniak, Eustace L., and Glenn D. Boreman. 1996. *Infrared Detectors and Systems*. New York.

Dial, Roman J, Gerard Q Ganey, and S McKenzie Skiles. 2018. "What Color Should Glacier Algae Be? An Ecological Role for Red Carbon in the Cryosphere." *FEMS Microbiology Ecology* 94 (3): fiy007. https://doi.org/10.1093/femsec/fiy007.

Duman, John G., and T.Mark Olsen. 1993. "Thermal Hysteresis Protein Activity in Bacteria, Fungi, and Phylogenetically Diverse Plants." *Cryobiology* 30 (3): 322–28. https://doi.org/10.1006/cryo.1993.1031.

Hamdan, Amira. 2018. "Psychrophiles: Ecological Significance and Potential Industrial Application." *South African Journal of Science* 114 (5–6): 1–6. https://doi.org/10.17159/sajs.2018/20170254.

Hanson, B. A. 2012. *ChemoSpec: Exploratory Chemometrics for Spectroscopy*. Version 6.1.4. https://bryanhanson.github.io/ChemoSpec/.

Ito, Shosuke, and Kazumasa Wakamatsu. 2008. "Chemistry of Mixed Melanogenesis--Pivotal Roles of Dopaquinone." *Photochemistry and Photobiology* 84 (3): 582–92. https://doi.org/10.1111/j.1751-1097.2007.00238.x.

Johansen, J. E., P. Nielsen, and C. Sjoholm. "Description of *Cellulophaga baltica* gen. nov., sp. nov. and *Cellulophaga fucicola* gen. nov., sp. nov. and Reclassification of [*Cytophaga*] *lytica* to *Cellulophaga lytica* gen. nov., comb. nov." *International Journal of Systematic Bacteriology* 49 (3): 1231–40. https://doi.org/10.1099/00207713-49-3-1231.

Jones, Robert M., Alison K. Thurston, Robyn A. Barbato, and Eftihia V. Barnes. 2020. *Evaluating the Conductive Properties of Melanin-Producing Fungus, Curvularia lunata, after Copper Doping*. ERDC TR-20-25. Hanover, NH: US Army Engineer Research and Development Center.

Jones, D., G. O. Ormondroyd, S. F. Curling, C.-M. Popescu, and M.-C. Popescu. 2017. "Chemical Compositions of Natural Fibres." In *Advanced High Strength Natural Fibre Composites in Construction*, edited by Mizi Fan and Feng Fu, 23–58. Sawston, UK: Woodhead Publishing. https://doi.org/10.1016/b978-0-08-100411-1.00002-9.

Kientz, Betty, Stephen Luke, Peter Vukusic, Renaud Péteri, Cyrille Beaudry, Tristan Renault, David Simon, Tâm Mignot, and Eric Rosenfeld. 2016. "A Unique Self-Organization of Bacterial Sub-Communities Creates Iridescence in *Cellulophaga lytica* Colony Biofilms." *Scientific Reports* 6: 19906. https://doi.org/10.1038/srep19906.

Lutz, Stefanie, Alexandre M. Anesio, Arwyn Edwards, and Liane G. Benning. 2015. "Microbial Diversity on Icelandic Glaciers and Ice Caps." *Frontiers in Microbiology* 6:307. https://doi.org/10.3389/fmicb.2015.00307.

Mariey, L., J. P. Signolle, C. Amiel, and J. Travert. 2001. "Discrimination, Classification, Identification of Microorganisms Using FTIR Spectroscopy and Chemometrics." *Vibrational Spectroscopy* 26 (2): 151–59. https://doi.org/10.1016/s0924-2031(01)00113-8.

Malik, K. A., N. A. Bhatti, and F. Kauser. 1979. "Effect of Soil Salinity on Decomposition and Humification of Organic Matter by Some Cellulolytic Fungi." *Mycologia* 71 (4): 811–20. https://doi.org/10.1080/00275514.1979.12021074.

Morita, R Y. 1975. "Psychrophilic Bacteria." *Bacteriological Reviews* 39 (2): 144–67. https://doi.org/10.1128/br.39.2.144-167.1975.

Mussagy, Cassamo Ussemane, James Winterburn, Valéria Carvalho Santos-Ebinuma, and Jorge Fernando Brandão Pereira. 2018. "Production and Extraction of Carotenoids Produced by Microorganisms." *Applied Microbiology and Biotechnology* 103 (3): 1095–1114. https://doi.org/10.1007/s00253-018-9557-5.

Nupur, L. N. U., Asheema Vats, Sandeep Kumar Dhanda, Gajendra P. S. Raghava, Anil Kumar Pinnaka, and Ashwani Kumar. 2016. "ProCarDB: A Database of Bacterial Carotenoids." *BMC Microbiology* 16:96. https://doi.org/10.1186/s12866-016-0715-6.

Ojeda, Jesús J., and Maria Dittrich. 2012. "Fourier Transform Infrared Spectroscopy for Molecular Analysis of Microbial Cells." In *Microbial Systems Biology*, edited by A. Navid, 187–211. https://doi.org/10.1007/978-1-61779-827-6_8.

Pati, Amrita, Birte Abt, Hazuki Teshima, Matt Nolan, Alla Lapidus, Susan Lucas, Nancy Hammon, et al.2011. "Complete Genome Sequence of *Cellulophaga lytica* Type Strain (LIM-21T)." *Standards in Genomic Sciences* 4 (2): 221–32. https://doi.org/10.4056/sigs.1774329.

Preisz, H. 1904. "Studien über Morphologie und Biologie des Milzbrandbacillus (mit besonderer Berücksichtigung der Sporenbildung auch bei anderen Bacillen)." *Zentralbl. Bakteriol. Parasitenkd. Orig* 35:280–293.

Rees, W G. 2001. *Physical Principles of Remote Sensing*. Cambridge, UK: Cambridge University Press.

R Core Team. 2017. *R: A Language and Environment for Statistical Computing*. Vienna, Austria: R Foundation for Statistical Computing. http://www.R-project.org/.

Schmitt, Jürgen, and Hans-Curt Flemming. 1998. "FTIR-Spectroscopy in Microbial and Material Analysis." *International Biodeterioration & Biodegradation* 41 (1): 1–11. https://doi.org/10.1016/s0964-8305(98)80002-4.

Smith, Brian. 2011. *Fundamentals of Fourier Transform Infrared Spectroscopy, Second Edition*. Boca Raton, FL:CRC Press.

Savitzky, Abraham, and M. J. E. Golay. 1964. "Smoothing and Differentiation of Data by Simplified Least Squares Procedures." *Analytical Chemistry* 36 (8): 1627–39. https://doi.org/10.1021/ac60214a047.

Stein, W. D. 1955. "Chemical Composition of the Melanin Granule and Its Relation to the Mitochondrion." *Nature* 175:256–57. https://doi.org/10.1038/175256a0.

Turick, Charles E., Amy A. Ekechukwu, Charles E. Milliken, Arturo Casadevall, and Ekaterina Dadachova. 2011. "Gamma Radiation Interacts with Melanin to Alter Its Oxidation–Reduction Potential and Results in Electric Current Production." *Bioelectrochemistry* 82 (1): 69–73. https://doi.org/10.1016/j.bioelechem.2011.04.009.

Yamashita, Yasuhiro, Norifumi Nakamura, Kazuhiro Omiya, Jiro Nishikawa, Hidehisa Kawahara, and Hitoshi Obata. 2002. "Identification of an Antifreeze Lipoprotein from *Moraxella* sp. of Antarctic Origin." *Bioscience, Biotechnology, and Biochemistry* 66 (2): 239–47. https://doi.org/10.1271/bbb.66.239.

Zhao, Qiao, Huanzhong Wang, Yanbin Yin, Ying Xu, Fang Chen, and Richard A. Dixon. 2010. "Syringyl Lignin Biosynthesis Is Directly Regulated by a Secondary Cell Wall Master Switch." *Proceedings of the National Academy of Sciences* 107 (32): 14496–501. https://doi.org/10.1073/pnas.1009170107.

Zhu, Lingli, Juha Suomalainen, Jingbin Liu, Juha Hyyppä, Harri Kaartinen, and Henrik Haggren. 2018. "A Review: Remote Sensing Sensors." *Multi-Purposeful Application of Geospatial Data*, edited by Rustam B. Rustamov, Sabina Hasanova and Mahfuza H. Zeynalova. London: IntechOpen. https://doi.org/10.5772/intechopen.71049.

Abbreviations

AFP	Antifreeze protein
ATCC	American Type Culture Collection
ATR	Attenuated total reflectance
ATR-FTIR	Attenuated total reflectance Fourier transform infrared
CRREL	US Army Cold Regions Research and Engineering Laboratory
EMR	Electromagnetic radiation
EMS	Electromagnetic spectrum
FTIR	Fourier transform infrared
ICE-COLD	Innovative, Collaborative, Exploratory Cold Regions Organismal Library for Discovery
IR	Infrared
KBr	Potassium bromide
LWIR	Long-wave infrared
MWIR	Midwave infrared
PC	Principle component
PCA	Principal component analysis
PDA	Potato dextrose agar
SPOT 5	Satellite Pour l'Observation de la Terre or "Satellite for Observation of Earth"

REPORT DOCUMENTATION PAGE

1. REPORT DATE	2. REPORT TYPE	3. DATES COVERED	
March 2023	Final Report	START DATE FY20	END DATE FY21

4. TITLE AND SUBTITLE
Characterization of Pigmented Microbial Isolates for Use in Material Applications

5a. CONTRACT NUMBER	5b. GRANT NUMBER	5c. PROGRAM ELEMENT
		0602144A
5d. PROJECT NUMBER	**5e. TASK NUMBER**	**5f. WORK UNIT NUMBER**
BN8	SBN811	

6. AUTHOR(S)
Elizabeth J. Corriveau, Travis L. Thornell, Mine G. Ucak-Astarlioglu, Dane N. Wedgeworth, Hayden A. Hanna, Robert M. Jones, Alison K. Thurston, and Robyn A. Barbato

7. PERFORMING ORGANIZATION NAME(S) AND ADDRESS(ES)
US Army Engineer Research and Development Center (ERDC)
Cold Regions Research and Engineering Laboratory (CRREL)
72 Lyme Road
Hanover, NH 03755-1290

ERDC Geotechnical and Structures Laboratory (GSL)
3909 Halls Ferry Road
Vicksburg, MS 39180-6199

8. PERFORMING ORGANIZATION REPORT NUMBER
ERDC TR-23-3

9. SPONSORING/MONITORING AGENCY NAME(S) AND ADDRESS(ES)	10. SPONSOR/MONITOR'S ACRONYM(S)	10. SPONSOR/MONITOR'S REPORT NUMBER(S)
Headquarters, US Army Corps of Engineers Washington, DC 20314-1000	USACE	

12. DISTRIBUTION/AVAILABILITY STATEMENT
DISTRIBUTION STATEMENT A. Approved for public release; distribution is unlimited.

13. SUPPLEMENTARY NOTES

14. ABSTRACT

Organisms (i.e., plants and microorganisms) contain pigments that allow them to adapt and thrive under stressful conditions, such as elevated ultraviolet radiation. The pigments elicit characteristic spectral responses when measured by active and passive sensors. This research study focused on characterizing the spectral response of three organisms and how they compared to background spectral signatures of a complex environment. Specifically, spectra were collected from a fungus, a plant, and two pigmented bacteria, one of which is an extremophile bacterium. The samples were measured using Fourier transform infrared spectroscopy and discriminated using chemometric means. A top-down examination of the spectral data revealed that organisms could be discriminated from one another through principal component analysis (PCA). Furthermore, there was a strong distinction between the plant and the pigmented microorganisms. Spectral differences resulting in samples with the highest variance from the natural background were identified using PCA loading plots. The outcome of this work is a spectral library of pigmented biological candidates for coatings applications.

15. SUBJECT TERMS
ATR-spectroscopy, Bacteria, Carotenoids, Coating analysis, FTIR-spectroscopy, Fungi, material analysis, Melanins, Microbial analysis, PCA, Pigments (Biology), Spectral sensitivity

16. SECURITY CLASSIFICATION OF:			17. LIMITATION OF ABSTRACT	18. NUMBER OF PAGES
a. REPORT	b. ABSTRACT	C. THIS PAGE		
Unclassified	Unclassified	Unclassified	SAR	35

19a. NAME OF RESPONSIBLE PERSON	19b. TELEPHONE NUMBER (include area code)